Magnetization moment recovery using Kelvin transformation and Fourier analysis

Laurent Baratchart, Juliette Leblond, Eduardo Andrade Lima, Dmitry Ponomarev

Magnetization moment recovery using Kelvin transformation and Fourier analysis

L. Baratchart[1], J. Leblond[1], E. A. Lima[2], D. Ponomarev[3,⋆]

[1] Projet APICS, INRIA, 2004 Route des Lucioles, 06902 Sophia Antipolis Cedex, France
[2] Earth, Atmospheric, and Planetary Sciences department, MIT, Cambridge, MA 02139, USA
[3] Laboratoire POEMS, ENSTA ParisTech, 828 Boulevard des Maréchaux, 91762 Palaiseau Cedex, France
⋆ Corresponding author

E-mail: dmitry.ponomarev@ensta-paristech.fr

Abstract. In the present work, we consider a magnetization moment recovery problem, that is finding integral of the vector function (over its compact support) whose divergence constitutes a source term in the Poisson equation. We outline derivation of explicit asymptotic formulas for estimation of the net magnetization moment vector of the sample in terms of partial data for the vertical component of the magnetic field measured in the plane above it. For this purpose, two methods have been developed: the first one is based on approximate projections onto spherical harmonics in Kelvin domain while the second stems from analysis in Fourier domain following asymptotic continuation of the data. Recovery results obtained by both methods agree and are illustrated numerically by plotting formulas for net moment components with respect to the size of the measurement area.

1. Introduction and problem formulation

Earth rocks and meteorites may preserve invaluable records of ancient planetary and solar nebula magnetic fields in the form of remanent magnetization. Recent advances in magnetometry (e.g., SQUID microscopy technique) have made it possible to measure magnetic fields of very low intensity generated by some rocks, and extraction of this relict magnetic information has become reality in cases that were previously inaccessible using standard rock magnetometers. An endeavor to develop a robust and efficient method for processing these data leads to a number of challenging problems such as effective extension of the restricted measurement data and extraction of certain features of the magnetization (typically, its mean value) that may still allow for retrieving those primordial records without having to solve the entire inverse problem for the underlying spatial distribution of magnetic sources. In particular, we are concerned with the following setting previously discussed in [2, 3].

Suppose there is a localized sample whose magnetization distribution is stationary and described by an unknown vector function

$$\vec{M}(\vec{x}) \equiv \left(M_1(\mathbf{x}, x_3), M_2(\mathbf{x}, x_3), M_3(\mathbf{x}, x_3)\right)^T, \quad \mathbf{x} \equiv (x_1, x_2)^T, \quad \vec{x} \equiv (\mathbf{x}, x_3)^T,$$

supported on a subset $Q \subset \mathbb{R}^3$.

Representation of the produced magnetic field in terms of the scalar potential Φ leads to the Poisson equation

$$\vec{B}/\mu_0 = -\nabla\Phi + \vec{M} \quad \Rightarrow \quad \Delta\Phi = \nabla\cdot\vec{M},$$

where $\mu_0 = 4\pi\cdot 10^{-7}$ H$\cdot$ m^{-1} is the magnetic constant. Therefore,

$$\Phi(\mathbf{x}, x_3) = -\frac{1}{4\pi}\iiint_{\mathbb{R}^3} \frac{\nabla\cdot\vec{M}(\vec{t})}{\left(|\mathbf{x}-\mathbf{t}|^2 + (x_3-t_3)^2\right)^{1/2}} d^3t.$$

In a typical experimental set-up, the vertical component of the magnetic field $B_3 = -\mu_0\frac{\partial}{\partial x_3}\Phi$ is measured on a part of the horizontal plane at height $x_3 = h > 0$

$$\begin{aligned} B_3(\mathbf{x}, h) &= \frac{\mu_0}{4\pi}\iiint_Q \left[3(h-t_3)\left(M_1(\vec{t})(x_1-t_1) + M_2(\vec{t})(x_2-t_2)\right)\right. \\ &\quad \left. + M_3(\vec{t})\left(2(h-t_3)^2 - |\mathbf{x}-\mathbf{t}|^2\right)\right] \frac{d^3t}{\left(|\mathbf{x}-\mathbf{t}|^2 + (h-t_3)^2\right)^{5/2}}. \end{aligned} \tag{1}$$

Then, knowing $B_3(\mathbf{x}, h)$ on some subset of the measurement plane above the sample, the main physical interest is to estimate the net magnetization moment vector of the sample

$$\vec{m} \equiv (m_1, m_2, m_3)^T := \iiint_Q \vec{M}(\vec{x})\, d^3x \in \mathbb{R}^3.$$

In the present work, we assume that this subset is a disk $D_A := \left\{\mathbf{x}\in\mathbb{R}^2 : |\mathbf{x}| \le A\right\}$.

2. Kelvin transform approach

2.1. Motivation of the method

Let us imagine the situation when we have available data for the potential on a sphere of radius $r = R_0$ encompassing the sample, i.e. the left-hand side of

$$\begin{aligned} \Phi(r,\theta,\phi) &= \frac{1}{4\pi}\iiint_Q \left[M_1(\vec{t})(r\sin\theta\cos\phi - t_1) + M_2(\vec{t})(r\sin\theta\sin\phi - t_2)\right. \\ &\quad \left. + M_3(\vec{t})(r\cos\theta - t_3)\right] \\ &\quad \times \frac{d^3t}{\left(r^2 - 2r\left[(t_1\cos\phi + t_2\sin\phi)\sin\theta + t_3\cos\theta\right] + t_1^2 + t_2^2 + t_3^2\right)^{3/2}}. \end{aligned} \tag{2}$$

Since Φ is harmonic for $r > R_0$, we can expand it over solid harmonics

$$\Phi(r,\theta,\phi) = \sum_{l=0}^{\infty}\frac{1}{r^{l+1}}\sum_{j=-l}^{l} c_{j,l} S_l^j(\theta,\phi), \quad S_l^j(\theta,\phi) := \begin{cases} P_l^j(\cos\theta)\cos(j\phi), & j \ge 0, \\ P_l^{|j|}(\cos\theta)\sin(|j|\,\phi), & j < 0, \end{cases}$$

where S_l^j are spherical harmonics and P_l^j are associated Legendre polynomials.

As seen from (2), Φ decays at infinity as $\mathcal{O}\left(1/r^2\right)$ which implies that $c_{0,0} = 0$.

Defining the L^2 inner product on the sphere of radius R in the usual way

$$\langle f, g\rangle_{L^2(\mathbb{S}_R)} = \int_0^{2\pi}\int_0^{\pi} f(r,\theta,\phi)\, g(r,\theta,\phi)\, R^2\sin\theta d\theta d\phi,$$

we employ orthogonality of spherical harmonics to obtain

$$\lim_{R\to\infty}\left\langle \Phi, \left(S_1^{-1}, S_1^0, S_1^1\right)^T\right\rangle_{L^2(\mathbb{S}_R)} = \left(-\frac{1}{3}m_2, \frac{1}{3}m_3, -\frac{1}{3}m_1\right)^T = \left(\frac{4\pi}{3}c_{-1,1}, \frac{4\pi}{3}c_{0,1}, \frac{4\pi}{3}c_{1,1}\right)^T,$$

that is,

$$m_1 = -3\left\langle \Phi, S_1^1\right\rangle_{L^2\left(\mathbb{S}_{R_0}\right)}, \quad m_2 = -3\left\langle \Phi, S_1^{-1}\right\rangle_{L^2\left(\mathbb{S}_{R_0}\right)}, \quad m_3 = 3\left\langle \Phi, S_1^0\right\rangle_{L^2\left(\mathbb{S}_{R_0}\right)}.$$

These formulas would exactly solve the moment recovery problem if we had the available data:

(i) on a sphere rather than on a horizontal plane;
(ii) for the potential rather than a component of the field;
(iii) on the complete surface rather than its subset.

To tackle the issue (i), we need to map the data to the sphere.

2.2. Kelvin transformation

Recall that in the complex plane $\mathbb{C}$, the Moebius transform $\frac{z-i}{z+i}$ sends the upper half-plane $\operatorname{Im} z > 0$ onto the unit disk $|z| < 1$ preserving harmonicity. Kelvin transformation is a generalization of this concept to higher dimensions [1]. In particular, we consider a one-parameter ($R_0 > 0$) family of transforms

$$\mathcal{K}[f]\left(\vec{\xi}\right) \equiv f^\star\left(\vec{\xi}\right) = \frac{1}{\left|\vec{\xi} - \vec{s}\right|} f\left(\mathcal{R}\vec{\xi}\right),$$

where $\vec{\xi} := (\xi_1, \xi_2, \xi_3)^T$, $\vec{s} := (0, 0, -R_0)^T$, $e_0 := \sqrt{2R_0\left(R_0 + h\right)}$, and

$$\mathcal{R}\vec{\xi} := \left(\frac{e_0^2\xi_1}{\xi_1^2 + \xi_2^2 + \left(\xi_3 + R_0\right)^2}, \frac{e_0^2\xi_2}{\xi_1^2 + \xi_2^2 + \left(\xi_3 + R_0\right)^2}, -R_0 + \frac{e_0^2\left(\xi_3 + R_0\right)}{\xi_1^2 + \xi_2^2 + \left(\xi_3 + R_0\right)^2}\right)^T,$$

which map functions on horizontal plane $x_3 = h$ onto those defined on the sphere of radius R_0 centered at the origin.

Hence, we have:

$$\Delta f\left(\mathbf{x}, x_3\right) = 0, \quad x_3 > h \qquad \Longleftrightarrow \qquad \Delta f^\star\left(\vec{\xi}\right) = 0, \quad \left|\vec{\xi}\right| < R_0.$$

Application of this transform to the potential followed by restriction to the sphere $\mathbb{S}_{R_0}$ gives

$$\begin{aligned}\mathcal{K}[\Phi](\theta,\phi) \;=\; & \frac{1}{4\pi R_0\sqrt{2\left(1+\cos\theta\right)}}\iiint_Q\left[M_1\left(\vec{t}\right)\left(\frac{\left(R_0+h\right)\sin\theta\cos\phi}{1+\cos\theta} - t_1\right)\right. \\ & \left. + M_2\left(\vec{t}\right)\left(\frac{\left(R_0+h\right)\sin\theta\sin\phi}{1+\cos\theta} - t_2\right) + M_3\left(\vec{t}\right)\left(h - t_3\right)\right] \\ & \times \frac{d^3t}{\left[\left(\frac{\left(R_0+h\right)\sin\theta\cos\phi}{1+\cos\theta} - t_1\right)^2 + \left(\frac{\left(R_0+h\right)\sin\theta\sin\phi}{1+\cos\theta} - t_2\right)^2 + \left(h - t_3\right)^2\right]^{3/2}}.\end{aligned}$$

Unfortunately, because of a more complicated angular dependence, the simple link between the net moment components and projections onto the first three spherical harmonics is now broken:

$$\left\langle \mathcal{K}\left[\Phi\right], S_1^{-1}\right\rangle_{L^2\left(\mathbb{S}_{R_0}\right)} \nsim m_1, \quad \left\langle \mathcal{K}\left[\Phi\right], S_1^{1}\right\rangle_{L^2\left(\mathbb{S}_{R_0}\right)} \nsim m_2, \quad \left\langle \mathcal{K}\left[\Phi\right], S_1^{0}\right\rangle_{L^2\left(\mathbb{S}_{R_0}\right)} \nsim m_3.$$

However, it turns out that proportionality in the first two formulas still holds asymptotically for large values of R_0 (as can be expected geometrically), that is, we again have

$$\lim_{R_0\to\infty} \left\langle \mathcal{K}\left[\Phi\right], S_1^{-1}\right\rangle_{L^2\left(\mathbb{S}_{R_0}\right)} \sim m_1, \quad \lim_{R_0\to\infty} \left\langle \mathcal{K}\left[\Phi\right], S_1^{1}\right\rangle_{L^2\left(\mathbb{S}_{R_0}\right)} \sim m_2.$$

Namely, multiscale analysis of integrals (see [4, Sect. 3.3.1]) results in

$$m_j = 6 \lim_{R_0\to\infty} R_0^4 \iint_{\mathbb{R}^2} \Phi\left(\mathbf{x}, h\right) \frac{x_j}{\left[x_1^2 + x_2^2 + \left(R_0 + h\right)^2\right]^{5/2}} dx_1 dx_2, \quad j = 1, 2.$$

Employing spherical harmonics expansion and a specially derived connection formula for normal derivatives

$$\mathcal{K}\left[\partial_{x_3}\Phi\right]\left(\vec{\xi}\right) = -\frac{1}{e_0^2}\left(R_0 + \xi_3\right)\left(\mathcal{K}\left[\Phi\right]\left(\vec{\xi}\right) + 2R_0\partial_r \mathcal{K}\left[\Phi\right]\left(\vec{\xi}\right)\right), \quad \vec{\xi} \in \mathbb{S}_{R_0},$$

we can show that

$$m_j = \frac{2}{\mu_0} \lim_{R_0\to\infty} R_0^5 \iint_{\mathbb{R}^2} B_3\left(\mathbf{x}, h\right) \frac{x_j}{\left[x_1^2 + x_2^2 + \left(R_0 + h\right)^2\right]^{5/2}} dx_1 dx_2, \quad j = 1, 2, \tag{3}$$

thus overcoming the issue (ii) from the previous subsection.

2.3. Normal component recovery and incomplete data

Interestingly enough, the normal component of the net moment cannot be recovered by asymptotic projection on the spherical harmonic S_1^0 neither from the field nor from the potential. One can, however, proceed another way. We use Poisson representation formula for $\mathcal{K}\left[\Phi\right]$ harmonic inside the ball and pass to the limit approaching vertically from inside the south pole $\vec{s}$ which, on the other hand, as an image of infinity under Kelvin transformation, must be proportional to m_3 at the leading order due to the dominance of vertical component term in the formula for B_3. Careful analysis and series of integrations by parts permitting passage to the limit lead to the following result [4, Sect. 3.4]

$$m_3 = -\frac{2}{\mu_0} \lim_{\rho\to\infty} \rho^3 \int_0^{2\pi} B_3\left(\rho\cos\varphi, \rho\sin\varphi, h\right) d\varphi. \tag{4}$$

Despite its simplicity, this formula is useless in practice for it only involves values of the field in the far region, exactly, where they cannot be measured.

We now focus on (iii), the last of the formulated issues, namely, dealing with incomplete data.

The remedy of situation for the case of normal component comes from application of Gauss theorem by splitting of the integral into a part with available values and its complement

$$0 = \iint_{\mathbb{R}^2} B_3\left(\mathbf{x}, h\right) dx_1 dx_2 = \iint_{D_A} B_3\left(\mathbf{x}, h\right) dx_1 dx_2 + \iint_{\mathbb{R}^2\setminus D_A} B_3\left(\mathbf{x}, h\right) dx_1 dx_2.$$

Assuming the measurement area D_A is large enough, we use, in the second term on the right, a far-distance asymptotic expansion of the field (1) whose integral is proportional to m_3. This immediately gives

$$m_3 = \frac{2}{\mu_0 A} \iint_{D_A} B_3(\mathbf{x}, h)\, dx_1 dx_2 + \mathcal{O}\left(\frac{1}{A^2}\right), \tag{5}$$

which provides a practical replacement of the formula (4).

Applying the same splitting and asymptotic extension strategy to (3), we arrive at

$$m_j = \frac{2}{\mu_0} \iint_{D_A} B_3(\mathbf{x}, h)\, x_j dx_1 dx_2 + \mathcal{O}\left(\frac{1}{A}\right), \quad j = 1, 2. \tag{6}$$

3. Fourier analysis

Define Fourier transform as $\mathcal{F}[f](\mathbf{k}) = \hat{f}(\mathbf{k}) = \iint_{\mathbb{R}^2} f(\mathbf{x}) e^{2\pi i \mathbf{k}\cdot\mathbf{x}} dx_1 dx_2$, $\mathbf{k} := (k_1, k_2)^T$, and observe that $\mathcal{F}\left[\left(x_1^2 + x_2^2 + H^2\right)^{-3/2}\right](\mathbf{k}) = \frac{2\pi}{H} e^{-2\pi H|\mathbf{k}|}$ for $H > 0$.

Then, representing the field as

$$\begin{aligned} B_3(\mathbf{x}, h) \;=\; & -\frac{\mu_0}{4\pi} \iiint_Q \left[(h - t_3) \left(M_1(\mathbf{t}, t_3) \left.\frac{\partial}{\partial x_1}\right|_{x_3 = h} + M_2(\mathbf{t}, t_3) \left.\frac{\partial}{\partial x_2}\right|_{x_3 = h} \right) \right. \\ & \left. + M_3(\mathbf{t}, t_3) \left.\frac{\partial}{\partial x_3}\right|_{x_3 = h} (x_3 - t_3) \right] \left(|\mathbf{x} - \mathbf{t}|^2 + (x_3 - t_3)^2 \right)^{-\frac{3}{2}} d^3 t, \end{aligned}$$

and denoting Q_3 the vertical projection of the magnetization support set Q, we take advantage of convolution structure of the integral operator and arrive at

$$\hat{B}_3(\mathbf{k}, h) = \pi \mu_0 \int_{Q_3} e^{-2\pi(h - t_3)|\mathbf{k}|} \left[i k_1 \hat{M}_1(\mathbf{k}, t_3) + i k_2 \hat{M}_2(\mathbf{k}, t_3) + |\mathbf{k}|\, \hat{M}_3(\mathbf{k}, t_3) \right] dt_3. \tag{7}$$

Note that $\vec{m} = \int_{Q_3} \hat{\vec{M}}(\mathbf{0}, t_3)\, dt_3$, and $\hat{\vec{M}}(\mathbf{k}, t_3)$ is smooth in $\mathbf{k}$ due to compact support of $\vec{M}$ (by Paley-Wiener theorem). Hence to extract the net moment information, we expand about $\mathbf{k} = \mathbf{0}$ all the right-hand side terms as well as the first integral in $\hat{B}_3(\mathbf{k}, h) = \left(\iint_{D_A} + \iint_{\mathbb{R}^2 \setminus D_A} \right) e^{2\pi i \mathbf{k}\cdot\mathbf{x}} B_3(\mathbf{x}, h)\, dx_1 dx_2$ and, in the second one, we use continuation of B_3 beyond the measurement area according to its asymptotics as discussed before. Matching terms of different smallness in $\mathbf{k}$, and employing asymptotic expansions of some special functions (Bessel, Struve, sine integral), we obtain a set of relations connecting field integrals against monomials with algebraic magnetization moments of different order (see [4, Sect. 3.6] for more details). In particular, taking the imaginary part of (7) and fixing either $k_1 = 0$ or $k_2 = 0$ we are led to formulas (6) whereas working with real part of (7) results in (5). More sophisticated combinations of the obtained relations yield asymptotic formulas which are superior to (6)

$$m_j = \frac{2}{\mu_0} \iint_{D_A} \left(1 + \frac{4x_j^2}{3A^2}\right) x_j B_3(\mathbf{x}, h)\, dx_1 dx_2 + \mathcal{O}\left(\frac{1}{A^2}\right), \quad j = 1, 2. \tag{8}$$

4. Numerical illustrations

We demonstrate results by performing numerical simulation on a synthetic example of few magnetic dipoles (i.e. point-supported magnetization sources) with positions $\vec{x}^{(1)} = (3.5, 3.0, 1.0)^T 10^{-5}$ m, $\vec{x}^{(2)} = (0.0, 0.0, 7.0)^T 10^{-5}$ m, $\vec{x}^{(3)} = (4.0, -5.5, 11.5)^T 10^{-5}$ m, $\vec{x}^{(4)} = (-4.0, 5.5, 2.5)^T 10^{-5}$ m and magnetic moments $\vec{m}^{(1)} = (4.5, 3.5, 1.0)^T 10^{-12}$ A·m^2, $\vec{m}^{(2)} =$

$(2.5, 4.5, 0.5)^T\, 10^{-12}$ A·m^2, $\vec{m}^{(3)} = (-3.0, 2.0, 2.5)^T\, 10^{-12}$ A·m^2, $\vec{m}^{(4)} = (-1.0, 2.0, 1.5)^T\, 10^{-12}$ A·m^2 producing a magnetic field measured at $x_3 = h = 2.5 \cdot 10^{-4}$ m.

Due to their asymptotic nature, the quality of the obtained formulas depends on the size of the measurement area: the bigger the area, the better the accuracy. We plot the estimates of the net moment components for different values of measurement disk radius A comparing the first and the second order accuracy formulas (6), (8) for the tangential components m_1, m_2, and illustrating the estimate for the normal component m_3 given by formula (5) which is already of the second order. Figure 1 contains results for the noiseless field whereas Figure 2 shows the same estimate for the field contaminated with Gaussian white noise of SNR=20 dB. We observe persistence of the estimates for m_1 and m_2 with respect to the noise while the estimate for m_3 has to be corrected to remedy amplification of noise due to factor A (in particular, we use 11-point linear regression to suppress asymptotically linear growth in A excluding from consideration the region of lower values of A). It is also clear that magnetic components of smaller magnitudes are more deteriorated by the noise.

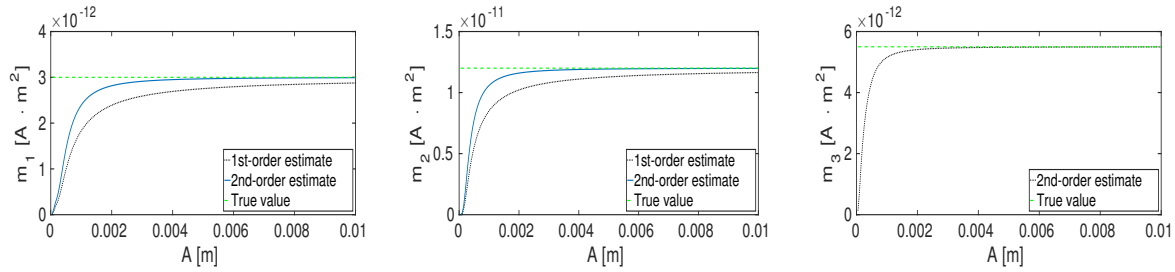

Figure 1. Estimates for m_1 (left), m_2 (center), m_3 (right) versus A, without noise.

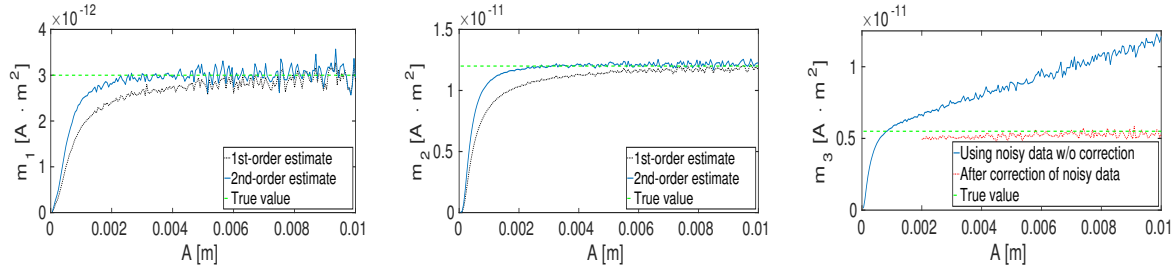

Figure 2. Estimates for m_1 (left), m_2 (center), m_3 (right) versus A, with noise of SNR=20.

5. Conclusion

The source feature (net moment vector) recovery issue in the context of inverse magnetization problem has been considered. We have devised two strategies of solving the problem which can be extended to more general frameworks. The second-order asymptotic formulas for estimating magnetization net moment components from the partially available data (5), (8) constitute the main practical outcome of the work. Residue terms in the obtained formulas can potentially be computed with arbitrary high precision and, by means of combination of measurements from different size areas, can be reduced to higher order of smallness. Some combinations of higher-order algebraic moments can also be easily extracted from the field data. The formulas extend to other geometries with the only difference being in numerical factors; in particular, rectangular geometry has been considered as well, and the corresponding results will be published elsewhere.

Acknowledgements
The authors would like to thank Doug Hardin (Vanderbilt University) and Sylvain Chevillard (INRIA Sophia Antipolis) for fruitful discussions.

References

[1] Axler S et al 2001 *Harmonic Function Theory* (New York: Springer-Verlag)
[2] Baratchart L, Hardin D P, Lima E A, Saff E B, Weiss B P 2013 Characterizing kernels of operators related to thin-plate magnetizations via generalizations of Hodge decompositions *Inverse Probl.* **29**(1)
[3] Lima E A, Weiss B P, Baratchart L, Hardin D P, Saff E B 2013 Fast inversion of magnetic field maps of unidirectional planar geological magnetization *J. Geophys. Res.: Solid Earth* **118**(6), 2723-52
[4] Ponomarev D 2016 *Some inverse problems with partial data*, PhD dissertation (University of Nice)